

ALIGNMENTS OF GROUP GALAXIES WITH NEIGHBORING GROUPS

YOUNGANG WANG¹, CHANGBOM PARK², XIAOHU YANG³, YUN-YOUNG CHOI⁴, XUELEI CHEN¹

Draft version May 31, 2018

ABSTRACT

Using a sample of galaxy groups found in the Sloan Digital Sky Survey Data Release 4, we measure the following four types of alignment signals: (1) the alignment between the distributions of the satellites of each group relative to the direction of the nearest neighbor group (NNG); (2) the alignment between the major axis direction of the central galaxy of the host group (HG) and the direction of the NNG; (3) the alignment between the major axes of the central galaxies of the HG and the NNG; and (4) the alignment between the major axes of the satellites of the HG and the direction of the NNG. We find strong signal of alignment between the satellite distribution and the orientation of central galaxy relative to the direction of the NNG, even when the NNG is located beyond $3r_{\text{vir}}$ of the host group. The major axis of the central galaxy of the HG is aligned with the direction of the NNG. The alignment signals are more prominent for groups that are more massive and with early type central galaxies. We also find that there is a preference for the two major axis of the central galaxies of the HG and NNG to be parallel for the system with both early central galaxies, however not for the systems with both late type central galaxies. For the orientation of satellite galaxies, we do not find any significant alignment signals relative to the direction of the NNG. From these four types of alignment measurements, we conclude that the large scale environment traced by the nearby group affects primarily the shape of the host dark matter halo, and hence also affects the distribution of satellite galaxies and the orientation of central galaxies. In addition, the NNG directly affects the distribution of the satellite galaxies by inducing asymmetric alignment signals. And NNG at very small separation may also contribute a second order impacts on the orientation of the central galaxy in the HG.

Subject headings: methods: statistical-galaxies: haloes-galaxies: structure-dark matter-large scale structure of universe

1. INTRODUCTION

The distribution of satellites in the groups of galaxies holds important clues to the assembly history of dark matter halos. Since satellite galaxies are typically distributed over the entire dark matter halo, they are a useful tracer of the dark matter distribution on the scale of the group. In particular, their position provides information on the shape of the dark matter halo (Carter & Metcalfe 1980; Plionis, Barrow & Frenk 1991; Fasano et al. 1993; Basilakos, Plionis & Maddox 2000; Orlov, Petrova & Martynova 2001; Plionis et al. 2004, 2006; Bailin & Steinmetz 2005; Wang et al. 2008, hereafter W08), and their kinematics could be used to estimate the mass of the haloes (e.g., Zaritsky et al. 1993, 1997; McKay et al. 2002; Brainerd & Specian 2003; Katgert, Biviano & Mazure 2004; van den Bosch et al. 2004; More et al. 2009a, 2009b).

One way to characterize quantitatively the distribution of satellite galaxies is to measure the alignment between their spatial distribution and the orientation of their central galaxies. Extensive studies with high-resolution simulations have shown that sub-haloes tend to align with the major axis of their host halos (Knebe et al. 2004,

2008a, 2008b; Libeskind et al. 2005, 2007; Wang et al. 2005; Zentner et al. 2005; Kang et al. 2007). The observational search for a possible alignment between the central galaxy and satellites has a long and serpentine history. The first study of such an alignment was performed by Holmberg (1969), who found that satellites are preferentially located along the minor axes of isolated disc galaxies. Holmberg's study was restricted to projected satellite-central distances of $r_p \lesssim 50$ kpc. Subsequent studies, however, were unable to confirm this so-called "Holmberg effect" (Hawley & Peebles 1975; Sharp, Lin & White 1979; MacGillivray et al. 1982). Zaritsky et al. (1997) studied the distribution of satellites around spiral hosts and were also unable to detect any significant alignment for $r_p \lesssim 200$ kpc, but they found a preferred minor-axis alignment for $300 \text{ kpc} \lesssim r_p \lesssim 500 \text{ kpc}$. The satellites of our Milk Way galaxy and the nearby M31 galaxy lie in planes which are highly inclined with respect to their discs. This was noted by Lynden-Bell (1976, 1982), Majewski (1994), Hartwick (1996, 2000) and Kroupa, Theis & Boily (2005) for the Milky Way, by Koch & Grebel (2006) and McConnachie & Irwin (2006) for M31, and by Metz, Kroupa & Jerjen (2007) for both galaxies.

With large redshift surveys, such as the 2dF Galaxy Redshift Survey (2dFGRS; Colless et al. 2001) and the Sloan Digital Sky Survey (SDSS; York et al. 2000), much larger samples of galaxy groups can be used to investigate this alignment problem. Sales & Lambas (2004; 2009) used a set of 1498 host galaxies with 3079 satellites from the 2dFGRS, and found a large-scale align-

¹ National Astronomical Observatories, Chinese Academy of Sciences, Beijing 100012, China; E-mail: wangyg@bao.ac.cn

² Korea Institute for Advanced Study, Dongdaemun-gu, Seoul 130-722, Korea; cbp@kias.re.kr

³ Key Laboratory for Research in Galaxies and Cosmology, Shanghai Astronomical Observatory, the Partner Group of MPA, Nandan Road 80, Shanghai 200030, China

⁴ Astrophysical Research Center for the Structure and Evolution of the Cosmos, Sejong University, Seoul 143-747, Korea

ment of the satellites along the host major axes for $300 \text{ kpc} \lesssim r_p \lesssim 500 \text{ kpc}$. Brainerd (2005) studied a sample of isolated SDSS galaxies, and found that the distribution of satellite galaxies is strongly aligned with the major axis of the disc host galaxy. Yang et al. (2006, hereafter Y06), using a galaxy group catalogue similar to the one used here, but based on the SDSS Data Release 2 (DR2), studied the alignment signal as a function of the color of the central and satellite galaxies. They found that the alignment strength is strongest between red centrals and red satellites, while the satellite distribution in systems with a blue central galaxy is consistent with being isotropic. Y06 also found that the alignment strength is stronger in more massive haloes and at smaller projected radii from the central galaxy. These results have subsequently been confirmed by several independent studies (Donoso, O’Mill & Lambas 2006; Azzaro et al. 2007; Agustsson & Brainerd 2006, 2007; W08; Steffen & Valenzuela 2008; Bailin et al. 2008). These studies have focused on whether the satellites are distributed along the major axis or minor axis of the central galaxy.

Besides the alignment between the distribution of satellite galaxies and the orientation of their central galaxy, other forms of alignment have also been studied. These include the alignment between neighboring clusters (Binggeli 1982; West 1989; Plionis 1994), between brightest cluster galaxies (BCGs) and their parent clusters (Carter & Metcalfe 1980; Binggeli 1982; Struble 1990), between the orientation of satellite galaxies and the orientation of the cluster (Dekel 1985; Plionis et al. 2003), and between the orientation of satellite galaxies and the orientation of the BCG (Struble 1990). Using the same group catalogue as the one used here, Faltenbacher et al. (2007) examined three different types of intrinsic galaxy alignment within groups: halo alignment between the orientation of the brightest group galaxies (BGG) and the distribution of its satellite galaxies, radial alignment between the orientation of a satellite galaxy and the direction toward its BGG, and direct alignment between the orientation of the BGG and that of its satellites. They found that the orientations of red satellites are preferentially aligned radially in the direction of the BGG. In addition, they found a weak but significant indication that the orientations of satellite galaxies are directly aligned with that of their BGG on scales $r < 0.1R_{\text{vir}}$. Based on a cosmological N -body simulation, Faltenbacher et al. (2008) analyzed the spatial and kinematic alignments of satellite halos within 5 times the virial radius of group-sized host halos. They found that the tidal forces on the large scales can give rise to a halo alignment out to at least $5R_{\text{vir}}$. This means that the alignment signal is strongly dependent on the large-scale environment. It is also found that the orientations of dark matter halos can be related to their surrounding structures, such as filaments and large-scale walls (e.g., Faltenbacher et al. 2002; Einasto et al. 2003; Avila-Reese et al. 2005; Hopkins, Bahcall & Bode 2005; Kasun & Evard 2005; Basilakos et al. 2006; Altay et al. 2006; Aragon-Calvo et al. 2006; Maulbetsch et al. 2007; Ragone-Figueroa & Plionis 2007; Hahn et al. 2007a, 2007b). Paz, Stasyszyn & Padilla (2008) used numerical simulations and the real data from the SDSS Data Release 6 (DR6) to study the alignments between the angular momentum of individual objects and the large-

scale structure. They found that the angular momentum of dark matter haloes are preferentially oriented in the direction perpendicular to the distribution of matter, and more massive haloes show a higher degree of alignment. Okumura, Jing & Li (2009) investigated the correlation between the orientation of giant elliptical galaxies, they measured the intrinsic ellipticity correlation function of 83773 SDSS luminous red galaxies (LRGs) and found that there is a positive alignment between pairs of the LRGs up to $30h^{-1}\text{Mpc}$ scales. Recently, Faltenbacher et al. (2009) used the SDSS DR6 and the Millennium simulation to determinate the alignment between galaxies and large-scale structure, and found that there is significant alignment between the major axes of red galaxies with the surrounding large-scale structure.

In this paper, we aim to study the impacts of the nearest neighbor groups (hereafter NNGs) and possibly the large scale environments beyond the NNGs (e.g., NNG has a higher probability to be distributed along the direction of the filament) on the various properties of the central and satellite galaxies, i.e., on the distribution of satellite galaxies and the shapes of the central and satellite galaxies. Throughout this paper, unless stated otherwise, when we refer to the impacts of the NNG, possible impacts from the large scale environments are not excluded. For our purposes, the following alignment signals are measured: (1) the alignment between the distributions of the satellites relative to the direction of the NNG; (2) the alignment between the major axis of the central galaxy of the host group (HG) and the direction of the NNG; (3) the alignment between the two major axes of the central galaxies of the HG and the NNG; and (4) the alignment between the major axes of the satellites of the HG and the direction of the NNG. Here the alignment signals (2), (3) and (4) are measured to probe the impact of the NNG on the shapes of the central and satellite galaxies, respectively.

This paper is organized as follows. In Section 2, we describe the observational data used for this study. Section 3 presents the method to quantify the alignment signal. Section 4 shows the results of various kinds of alignment signals we measured, and their dependence on the morphology of the central galaxies of the HG and the NNG. Section 5 summarize our results and discuss various related issues.

2. OBSERVATIONAL DATA SET

2.1. Groups: central and satellite galaxies

The analysis presented in this paper is based on the SDSS DR4 galaxy group catalogue of Yang et al. (2007)⁵. This group catalogue is constructed by applying the halo-based group finder of Yang et al. (2005) to the New York University Value-Added Galaxy Catalogue (NYU-VAGC; see Blanton et al. 2005), which is based on the SDSS DR4 (Adelman-McCarthy et al. 2006). From this catalogue Yang et al. selected all galaxies in the Main Galaxy Sample with redshifts in the range $0.01 \leq z \leq 0.20$ and with a redshift completeness greater than 0.7. This sample of galaxies is further divided into three group samples: sample I, which only uses the 362, 356 galaxies

⁵ In this paper, we refer to systems of galaxies as groups regardless of their richness, including isolated galaxies (i.e., systems with a single member) and rich clusters of galaxies.

with measured redshifts from the SDSS; sample II, which also includes 7091 galaxies with SDSS photometry but with redshifts taken from alternative surveys; and sample III, which includes an additional 38,672 galaxies which do not have measured redshifts due to fiber-collision, but were assigned the redshift of nearest neighbors (cf. Zehavi et al. 2002). The present analysis is based on the sample II, which consists of 369,447 galaxies distributed over 301,237 groups with a sky coverage of 4514 deg^2 . Details of the group finder and the general properties of the groups can be found in Yang et al. (2007).

The halo mass of each group is estimated using the ranking of the group's characteristic stellar mass, M_{stellar} , defined as the total stellar masses of all group members with absolute magnitude $^{0.1}M_r - 5 \log h \leq -19.5$. More details of the mass estimations can be found in Yang et al. (2007). For those groups with all members that have absolute magnitudes $^{0.1}M_r - 5 \log h > -19.5$, which are not assigned halo masses in the group catalogue, we use the mean stellar-to-halo mass relation obtained in Yang et al. (2009) to assign their halo masses. In this study, only groups with halo masses $M \geq 10^{11.5} h^{-1} M_{\odot}$ are selected. Note also that in these group catalogues the survey edge effects have been taken into account (Yang et al. 2007). We use only those groups with $f_{\text{edge}} \geq 0.6$, where $1 - f_{\text{edge}}$ is the fraction of galaxies in a group that are missed due to the survey edges.

Applying all the above mentioned selection criteria (magnitude, mass and f_{edge}), we have a total of 27,173 central galaxies and 64,366 satellite galaxies. Here the central galaxy is defined to be the most massive (in terms of stellar mass) galaxy in each group and other galaxies are satellites. These galaxies are used to detect the first kind of alignment signals where position angles of galaxies are not required.

However, in order to study other three kinds of alignment signals, the position angles of the galaxies are required. For these studies, we keep only those galaxies with $b/a < 0.75$ whose isophotal position angles are well defined. Here a and b are the isophotal semi-major and minor axis lengths, respectively. Thus within our final sample with 27,173 central and 64,366 satellite galaxies, 13,890 central and 44,219 satellite galaxies have well measured position angles.

Finally, note that the selected galaxy groups contain some interlopers, i.e. false members assigned to a group. If the distribution of these interlopers is uncorrelated (or anti-correlated) with that of the true members of the group, our results on the first kind of alignment would be negatively biased. According to Yang et al. (2007; 2005) the average fraction of interlopers in the group is less than 20%. We have tested the effects of such interlopers by assuming that the distribution of the interlopers is uncorrelated with the shape of the group and is spherical, and found that the presence of the interlopers can decrease the first type of the alignment signal by $\sim 10\%$.

2.2. Galaxies: early and late types, position angles

In our study we follow the prescription of Park & Choi (2005) to divide our sample into the early (ellipticals and lenticulars) and the late (spirals and irregulars) morphological types. This division is based on their location in the $u - r$ versus $g - i$ color gradient space, and also in the

i -band concentration index space. The early type galaxies are classified as those lying above the boundary lines passing through the points (3.5, -0.15), (2.6, -0.15), and (1.0, 0.3) in the $u - r$ versus $\Delta(g - i)$ space. They are also required to have the (inverse) concentration index $c \equiv R_{50}/R_{90} < 0.43$, where R_{50} and R_{90} are the radii from the center of galaxy containing 50% and 90% of the Petrosian flux. The rest of the galaxies are classified as late-type galaxies. The completeness and reliability of this classification scheme reaches 90%. For more details of the morphology classification, we refer the reader to Park & Choi (2005). In this paper, we adopt the r band isophotal position angle for each galaxy, which is given in the SDSS-DR4 (Adelman-McCarthy et al. 2006). We have checked the distributions of these position angles and found them to be isotropic.

2.3. The nearest neighbor group

A very important step in our investigation is to find the nearest neighbor group, so that we can define/estimate the direction of the tidal force. Here we combine the pairwise velocity differences and the projected distances between the central galaxies of the HG and its neighboring groups in selecting the nearest neighbor. Note that the *pairwise velocity differences* here refers to the line-of-sight velocity difference between the two central galaxies of the groups. For a given host group, its NNG is found in the following way.

We first inspect the distribution of the pairwise velocity difference between central galaxies of the HG and the neighboring groups to set up the velocity difference criteria (e.g., Park & Choi 2009). Figure 1 shows the distribution of the velocity difference Δv for the early (filled dot) and late (open circle) type centrals. These profiles are obtained by measuring the velocity difference Δv distribution of all central galaxy pairs with the projected distance r_p between 0.4 and $1 h^{-1} \text{ Mpc}$. Note that these profiles are contributed by two components: (1) the randomly distributed, un-correlated pairs (constant component); and (2) the correlated pairs (e.g., by neighbor groups; enhanced component). Since the impact of pairwise *peculiar* velocity of galaxies is to broaden the distribution of the correlated pairs, we may use the measured profile to probe the *up-limit* of the pairwise peculiar velocity assuming that the correlated pairs in real space have a very compact distribution.

According to the measured Δv distribution shown in Figure 1, we fit to the data using an exponential function plus a constant:

$$f(\Delta v) = f_1 \exp(-\Delta v / \sigma_{\Delta v}) + f_2, \quad (1)$$

where f_1 , f_2 and $\sigma_{\Delta v}$ are fitting parameters. The best fit characteristic (*up-limit*) velocity differences $\sigma_{\Delta v}$ are 342 and 243 km/s for early and late type centrals, respectively, and the fitting curves are shown as the solid (early type) and dashed (late type) lines in Figure 1.

We use the following criteria to select the NNG: (1) for a given central galaxy of a HG, if the central galaxy of the neighbor group has velocity difference less than 800 (for early type central) or 600 (for late-type central) km/s (about 2.4 times the characteristic velocity difference) and projected separation $r_p < 3 h^{-1} \text{ Mpc}$, the neighbor with the smallest r_p is set as the NNG; (2) if there is no central galaxy within the velocity difference

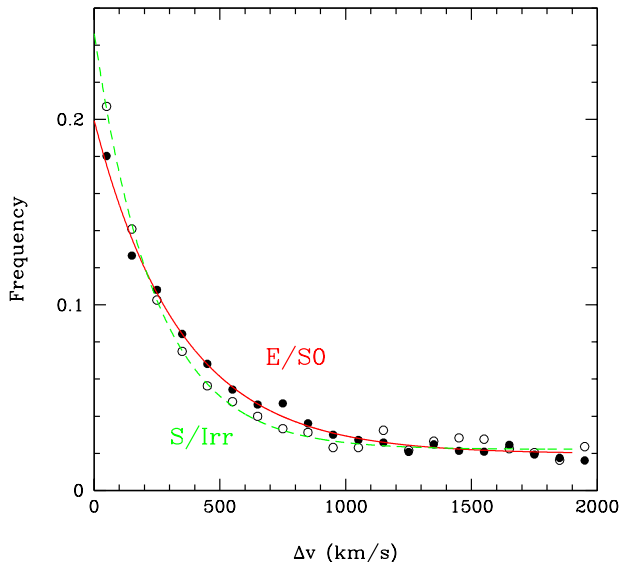


FIG. 1.— Probability distribution of the velocity difference Δv between early (filled dot) or late (open circle) type centrals and other central galaxies at projected separation $r_p = 0.4 \sim 1 h^{-1} \text{Mpc}$. The solid line is the best fit curve for the early (E/S0) morphological type centrals, while the dashed one is for the late (S/Irr) type centrals.

or r_p limit, the neighbor with the smallest three dimensional separation s is set to as the NNG, since this group has a higher probability of being the true NNG in real space than the other ones with smaller r_p but beyond the velocity difference limit. These velocity values (800 km/s and 600 km/s, roughly 2.4 times the characteristic velocity difference) are chosen as a reasonable compromise between obtaining a large sample and reducing the fraction of interlopers in the sample. Since the line-of-sight pairwise peculiar velocity of galaxies is typically 300 km/s (see Figure 1), it is very unlikely for redshift distortion to make real space close pairs to be separated in redshift space with velocity difference much larger than 300 km/s, so the three dimensional distance in redshift space between the two central galaxies can be used as the distance indicator. On the other hand, the central galaxy pairs with velocity difference less than 800 km/s (early types) or 600 km/s (late types) and r_p less than $3h^{-1} \text{Mpc}$ are modeled using the projected separation r_p as the distance indicator. However, we have checked varying these velocity differences (800 km/s for early type and 600 for late-type) and found that our results are not sensitive to the exact values used. Finally, note that one can also define the NNG according to the projected separation relative to the size of the host group (e.g., its virial radius). However, we have made tests and again found that using such an alternative definition of the NNG will not have any significant impact on our results.

3. QUANTIFYING THE ALIGNMENT

To study the impacts of the NNG on the various properties of the central and satellite galaxies, we first measure the different alignment signals as we listed in Section 1. The alignments of objects are obtained by computing the distribution functions of the alignment angles (e.g., Brainerd 2005), $P(\theta_i)$ ($i = 1, 2, 3, 4$), where θ_i is the angle between the two directions.

The angle θ_1 is the projected angle between the line

connecting the central galaxy to the satellite galaxy and the line connecting the central galaxy to the NNG (See the left panel of Figure 2). The angle θ_1 is constrained in the range $0^\circ \leq \theta_1 \leq 180^\circ$, where $\theta_1 < 90^\circ$ ($> 90^\circ$) implies a satellite is at the near (far) side of the HG with respect to the NNG. We also define an angle

$$\tilde{\theta}_1 \equiv \begin{cases} \theta_1, & \theta_1 < 90^\circ \\ 180^\circ - \theta_1, & \theta_1 > 90^\circ \end{cases} \quad (2)$$

The range of $\tilde{\theta}_1$ is $0^\circ \leq \tilde{\theta}_1 \leq 90^\circ$, which is more useful when making average.

The angle θ_2 is the angle between the major axis of the central galaxy of the HG and the direction of the NNG (See the left panel of Figure 2), which is constrained to be in the range $0^\circ \leq \theta_2 \leq 90^\circ$. $\theta_2 = 0^\circ$ (90°) suggests that the major (minor) axis of the central galaxy of the HG is perfectly aligned with the direction of the NNG.

The angle θ_3 is the angle between the two major axes of the central galaxies of the HG and the NNG. As shown in Figure 3, the angular separations between HG and NNG on the celestial sphere can reach up to 2° for some pairs, so for the sake of accuracy, we have included the curvature effect in the determination of θ_3 by parallel transport the angles along great circles on the celestial sphere. The procedure is illustrated in the right panel of Figure 2, and explained in more details in the Appendix. Note however that neglecting this effect does not have any significant impact on our results. The angle θ_3 is also constrained in the range $0^\circ \leq \theta_3 \leq 90^\circ$.

The angle θ_4 is similar to θ_2 but defined for the major axes of the satellite galaxies, i.e., the angle between the major axis of the satellite galaxy of the HG and the direction of the NNG.

In the following we will take θ_1 as an example to explain the process of measuring the alignment signals, the measurement of $\theta_2, \theta_3, \theta_4$ are similar.

For a given set of the HG-NNG pairs, we first count the number of satellite-central-NNG pairs, $N(\theta_1)$, that have the angle θ_1 between the central-satellite direction and the direction of the NNG in a number of θ_1 bins. Next, we construct 100 random samples in which we randomize the positions of all NNGs, and compute $\langle N_R(\theta_1) \rangle$, the average number of satellite-central-NNG pairs for the randomly located NNGs as a function of θ_1 . The random samples constructed this way suffer exactly the same selection effects as the real sample, so any significant difference between $N(\theta_1)$ and $N_R(\theta_1)$ reflects a genuine alignment between the distribution of the satellite galaxies in the HG and the direction of the NNG.

Following Y06 and W08, we quantify the alignment signal by using the distribution of normalized pair counts:

$$f_{\text{pairs}}(\theta_1) = \frac{N(\theta_1)}{\langle N_R(\theta_1) \rangle}. \quad (3)$$

In the absence of any alignment, $f_{\text{pairs}}(\theta_1) = 1$, while $f_{\text{pairs}}(\theta_1) > 1$ near $\theta = 0$ or 180 degree implies a satellite distribution preferentially aligned along the direction of the NNG.

We may quantify the fluctuation using $\sigma_R(\theta_1)/\langle N_R(\theta_1) \rangle$, where σ_R is the standard deviation of $N_R(\theta)$, which could be estimated from the 100

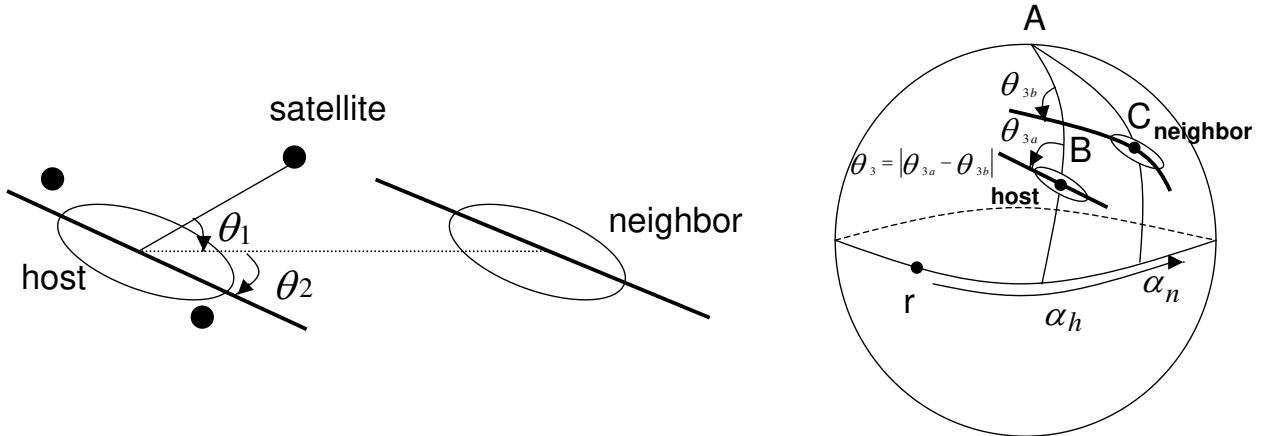


FIG. 2.— Illustration of the first three alignment angles θ_1 , θ_2 (left panel) and θ_3 (right panel).

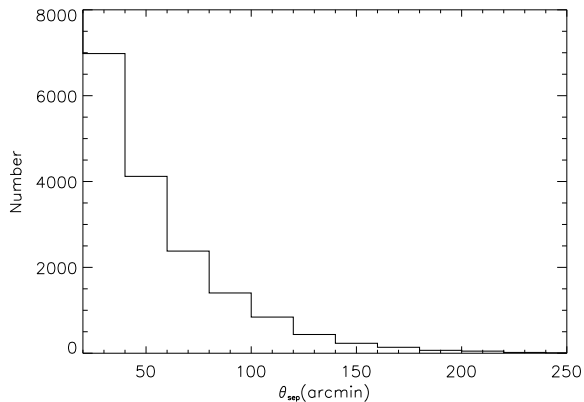


FIG. 3.— The distribution of angular separations between HGs and NNGs for our sample.

random samples. In addition to this normalized pair count, we also compute the average angle $\langle \theta_1 \rangle$. In the absence of any alignment $\langle \tilde{\theta}_1 \rangle = 45^\circ$. If one finds $\langle \tilde{\theta}_1 \rangle < 45^\circ$ ($\langle \tilde{\theta}_1 \rangle > 45^\circ$), it means that the satellites

are parallel (perpendicular) to the line connecting the host-neighbor pairs.

4. RESULTS

4.1. Satellite galaxy distribution relative to the direction of the NNG

As have been found in recent papers, the satellite galaxies are distributed preferentially along the major axis of the central galaxies, especially those with red central galaxies (e.g., Brainerd 2005; Agustsson & Brainerd 2006; Y06; Azzaro et al. 2007; Kang et al. 2007; W08). This shows that the distribution of the satellite galaxies is not completely random, but is correlated with the shapes of the central galaxies. In this subsection we check whether similar correlations exist beyond the single dark matter halo of the group. In order to describe the deviation of the alignment signal from the null, a χ^2 test is applied here

$$\chi^2 = \sum_{i=1}^{N_{\text{bin}}} \frac{(f_{\text{pairs}} - 1.0)^2}{\sigma_{\text{R}}^2} \quad (4)$$

where N_{bin} denotes the bin number of the angular distribution.

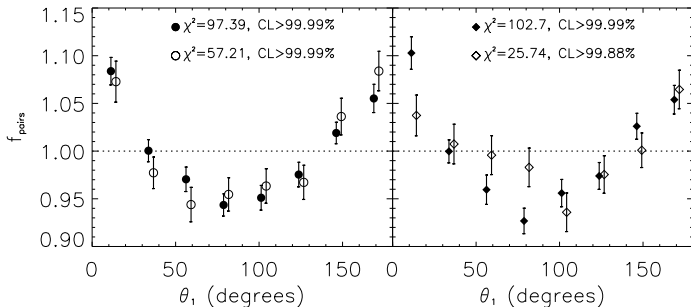


FIG. 4.— The normalized probability distribution for θ_1 , the angle between the directions of the satellite galaxies in the HG and the NNG. The left panel shows results for the whole sample (filled circle) and the subsample with projected distance smaller than $3r_{vir}$ of the host group (open circle). The right panel shows results for the subsamples where the mass of the HG are larger (filled diamond) and smaller (open diamond) than that of the NNG. The open symbols are shifted slightly along the horizontal axis for clarity.

The filled circles in the left-hand panel of Figure 4 shows the distribution of $f(\theta_1)$ for all satellite-NNG pairs in our SDSS group catalogue. One can see that $f_{pairs}(\theta_1) > 1$ at small (near 0°) and large θ_1 (near 180°) values, while it is less than 1 at middle values (near 90°). From the figure, we see clearly that the distribution of HG satellites are not completely uniform or isotropic, there is a small (in absolute strength) but highly significant preference for the direction along the line connecting HG and NNG. The deviation from uniform distribution has $\chi^2 = 97.39$, corresponding to $CL > 99.99\%$ for 8 degree of freedom (hereafter dof). The average value of θ_1 is $\langle \theta_1 \rangle = 43.8^\circ \pm 0.1^\circ$, which again shows that the distribution of satellites of HG are not isotropic or uniform, but slightly prefers the direction of the NNG. The effect is small but highly significant ($\sim 10\sigma$). For comparison, the open circle in the left panel of Figure 4 shows $f_{pairs}(\theta_1)$ for the host-neighbor pairs with the projected distance smaller than 3 times of the virial radius of the HG. There is no significant difference between the filled circle and open circle lines, the confidence of this difference is below 0.5σ level. *In other words, not only the NNGs but also the large scale environments, e.g. the filaments, represented by the NNGs that affect (or at least play an important role in) the distribution of the satellites (and the mass distribution within the host halo).* Otherwise we would expect distance dependent signals.

Note that in the above discussion, the NNG can be either more massive or less massive than the HG, it may be interesting to investigate these two cases separately. For this purpose, in the right-hand panel of Figure 4 we show the resulting θ_1 distributions for HG-NNG systems with the mass of HG larger (filled diamond) and smaller (open diamond) than that of the NNG. In the rest part of the paper, unless stated otherwise, we use filled circle symbol to represent the sample which is not constrained by the distance limit while the open circles to represent the results with the projected distance smaller than 3 times

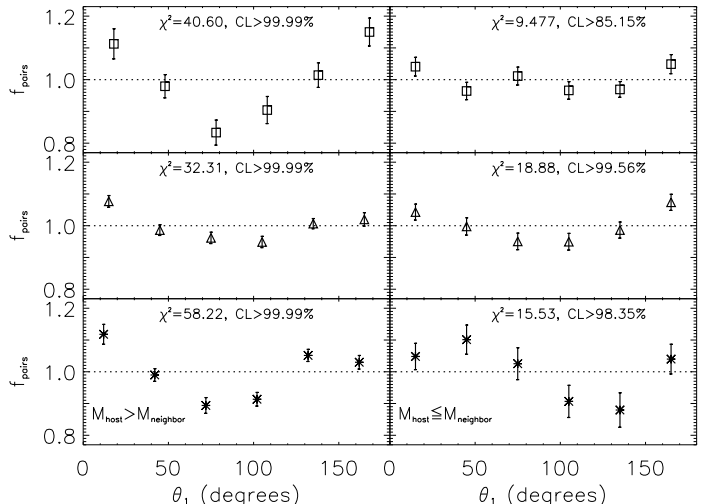


FIG. 5.— Similar to Fig. 4, but here for different HG-NNG systems. Left panels: results for HG-NNG systems where the mass of the HG is larger than that of the NNG. Right panels: results for HG-NNG systems where the mass of the HG is smaller than that of the NNG. The asterisk, triangle and square symbols represent the mass of the NNG in the range $M_n \in [11.5, 12.5]$, $[12.5, 13.5]$ and $[13.5, 14.5]$, respectively.

the virial radius of the HG; the filled diamond (open diamond) symbol represents the results for subsamples where the mass of the HG are larger (smaller) than that of the NNG. The stronger alignment signals shown in the right-hand panel in Figure 4 for satellite galaxies in more massive HGs may caused by the fact that their distributions are flatter than those in smaller HGs (e.g., Jing & Suto 2002; Yang et al. 2006).

We can further check this by measuring the alignment signals for HG-NNG systems that are divided into subsamples of different masses. In the left panel of Figure 5, we show the alignment signal of $f_{pairs}(\theta_1)$ for the submaples with mass of the HG that are larger than that of the NNG, while in the right panel of the Figure 5, we show the results of the subsamples with the mass of the HG smaller than that of the NNG. In each panel, the asterisk, triangle and square symbols represent the mass of the NNG in the range $M_n \equiv \log_{10}(hM/M_\odot) \in [11.5, 12.5]$, $[12.5, 13.5]$ and $[13.5, 14.5]$, respectively. We found some interesting trends here. According to the left panel of Figure 5, for the most massive groups ($M_n > 13.5$), the alignment signal (i.e. deviation of $f_{pairs}(\theta_1)$ from 1) is strongest (5σ), perhaps indicating the very strong attraction by the NNG and the flatter distribution of satellite galaxies within the HG. For system with less massive HG and NNGs ($M_n \in [12.5, 13.5]$), the signal is weaker (deviation from null signal hypothesis by 3σ). However, for the smallest groups discussed here ($M_n \in [11.5, 12.5]$), the alignment signal is again rather strong (deviation from null signal hypothesis by 5σ). This is also evident from the value of χ^2 , 58.22, 32.31, 40.60, corresponding to the mass of the NNG in the range $M_n \in [13.5, 14.5]$, $[12.5, 13.5]$ and $[11.5, 12.5]$, respectively. Interestingly, for those systems with NNG heavier than HG and NNG in the range $M_n \in [11.5, 12.5]$ (bottom right panel), there are slightly more satellite galaxies distributed near the NNG (with $\theta_1 < 90^\circ$) than HG (the confidence level is 1.5σ), which may indicate that the NNG near a small HG may attract its satellite

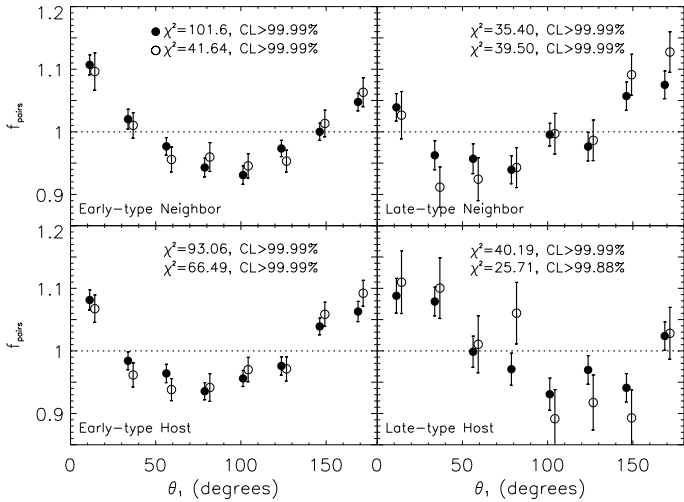


FIG. 6.— Same as Fig. 4, but for different subsamples, divided by the type of the central galaxies of the HG or NNG.

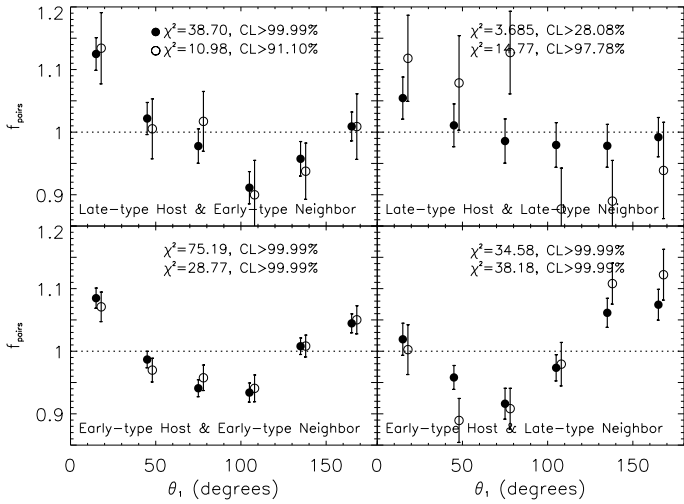


FIG. 7.— Same as Fig. 6, except that here we split the sample according to the morphological types of both the central galaxies of the HG and NNG.

galaxies and affect their distribution.

In order to study how this alignment depends on the morphological types of the central galaxies of the HG and the NNG, following Y06 and W08, we divide our sample of host and neighbor groups into different morphology subsamples. Figure 6 shows the alignment signals $f_{\text{pairs}}(\theta_1)$ for HG with early (lower-left panel) and late-type (lower-right panel) central galaxy, and NNG with early (upper-left panel) and late-type (upper-right panel) central galaxy, respectively.

The alignment signal does seem to depend on the morphological type of the central galaxy slightly: the groups with early type central galaxies or with the NNGs having an early central galaxy show slightly stronger alignment than those with late-type centrals (1.0σ for the early centrals of HG than late centrals of HG, 1.7σ for the early centrals of NNG than late centrals of NNG). In Figure 7, we show the alignment, $f_{\text{pairs}}(\theta_1)$, for four combinations of the HG and NNG with central galaxies of different morphological types. As one can see, pairs with the late-type HG and late-type NNG show the smallest strength of the alignment signal.

The HG satellite distribution is also slightly asymmet-

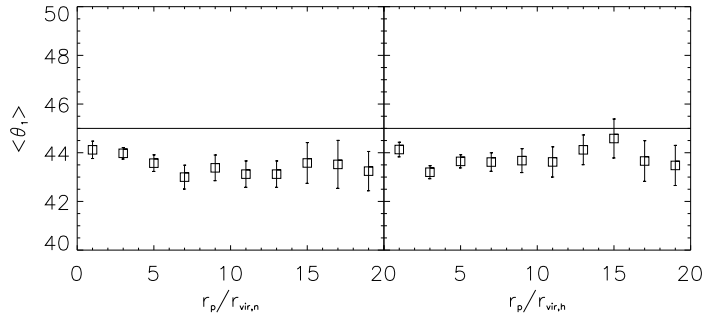


FIG. 8.— The average value of θ_1 as a function of the projected distance between the HG and the NNG. Left: as a function of $r_{p,n}$; Right: as a function of $r_{p,h}$.

ric with respect to the near side or far side from the NNG. There is a small but significant preference for the satellite galaxies in a group with a late type central galaxy to be distributed near the side of the NNG, with either an early or a late type central galaxy. This asymmetry is significant by $\sim 2\sigma$ for both the whole sample and for the case where the NNG with projected separation is smaller than 3 times of the virial radius. For the samples with the early-type HG and late-type NNG, however, the trend is opposite: the satellite galaxies are preferentially distributed on the far side from the NNG, again this effect is small but significant (2.4σ for all samples, 2.7σ for the close pairs). The reason of this is not completely clear, but it may be due to (i) the groups with late type central galaxy is more probably located in the outskirts of a high density region with groups having preferentially early type central galaxies; (ii) probably smaller than groups with early type central galaxies, thus have smaller impact on its NNG. Before we proceed, it is quite interesting to check whether or not the weak asymmetry is induced by those groups near the survey edges. As we have tested using only groups with $f_{\text{edge}} > 0.9$ by performing exactly the same analysis, the weak asymmetry is almost the same. Moreover, one would only expect that the groups near the edge may slightly induce the weak asymmetry in the direction of the *near* side of the NNG, however not in the *far* side of the NNG, as shown in the lower-right panel of Figure 7. Therefore, we believe that our results (e.g., the weak asymmetry) are robust against the impact of groups near the survey edges.

To what extent does the large scale environment as represented by the NNG affect the distribution of the satellite galaxies in the HG? To study this problem, we divided the total sample into subsamples according to the projected distance between the HG and the NNG. Figure 8 shows the dependence of the average value θ_1 on the projected distance between the HG and the NNG. Here we take both the virial radius of the NNG, $r_{\text{vir},n}$ (left panel), and the HG, $r_{\text{vir},h}$ (right panel), as the unit. There is no significant difference between the results in the left and right panels. The value of $\langle\theta_1\rangle$ depends weakly on the distance between the HG and NNG. The alignment between the distribution of satellite galaxies

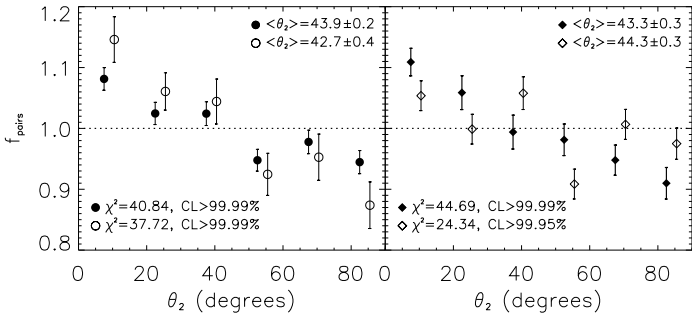


FIG. 9.— The normalized probability distribution, $f_{\text{pairs}}(\theta_2)$, of the angle θ_2 between the major axes of the central galaxy of the HG and the direction of the NNG. In the left panel, results are measured for all samples (filled circle) and the subsamples with the projected distance smaller than 3 times the virial radius of the host group (open circle). In the right panel, we show results for subsamples where the mass of the HG are larger (smaller) than that of the NNG with filled diamond (open diamond) symbol. Formal rejection confidence levels from the χ^2 test are shown in each panel. The open circles and open diamonds have been shifted slightly along the horizontal axis for clarity.

and the direction of the NNG is significant (greater than 1σ) up to separations as large as about $12r_{\text{vir},n}$ (or $r_{\text{vir},h}$), which is also evident from the fact that $\langle\theta_1\rangle = 43.1^\circ \pm 0.5^\circ$ (or $43.6^\circ \pm 0.6^\circ$) for the systems with separation of the HG and the NNG being $12r_{\text{vir},n}$ (or $r_{\text{vir},h}$). From these alignment signals for θ_1 at so large separations, we conclude that the distributions of the satellite galaxies in HGs are (also) affected by the large scale environments.

4.2. The position angle of the central galaxy

4.2.1. relative to the direction of the NNG

Both Y06 and W08 found that there is a preference for the satellites to be distributed along the major axis of their central galaxy, and in the previous section, we found a prominent alignment signal between the orientation of the satellite system of the HG and the direction of the NNG. Therefore, we expect there is also an alignment between the major axis of the central galaxy of the HG and the direction of the NNG.

Indeed, as shown in the left panel of Figure 9, there is a strong signal of alignment between these two directions: the major axis of the central galaxy of the HG is preferentially aligned with the direction of the NNG. The alignment signal is even stronger for the pairs with smaller projected separations as shown by the open circle symbols of Figure 9. This result suggests that the major axis of the central galaxy of the HG tends to be aligned with the direction of the NNG (or possibly the large scale structure beyond).

The orientation of the central galaxy of HG is possibly affected by (1) the potential of the HG; (2) NNG and (3) the large scale environment. To understand the relative influence of these factors, we checked separately the signals for all pairs of NNG and the close pairs ($\leq 3r_{\text{vir}}$), and find the following average values: $\langle\theta_2\rangle = 43.9^\circ \pm 0.2^\circ$ ($\langle\theta_2\rangle = 42.7^\circ \pm 0.4^\circ$ for the close pairs), which depend

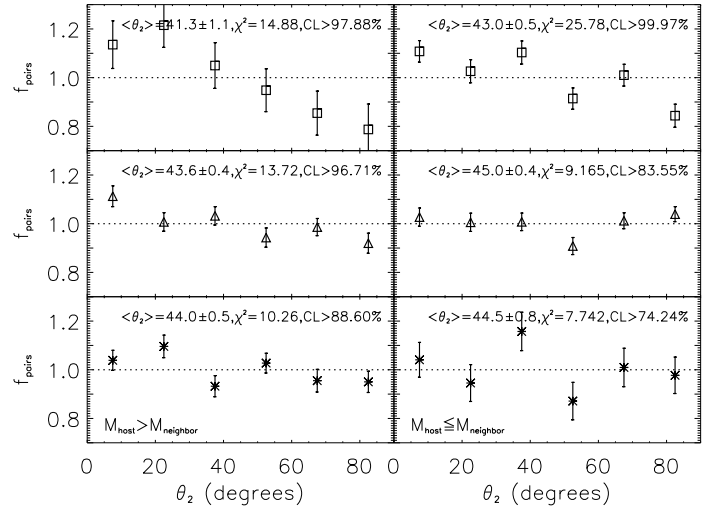


FIG. 10.— Similar to Fig. 9, but here for different HG-NNG systems. Left panels: results for HG-NNG systems where the mass of the HG is larger than that of the NNG. Right panels: results for HG-NNG systems where the mass of the HG is smaller than that of the NNG. In each panel, the asterisk, triangle and square points represent the mass of the NNG in the range $M_n \in [11.5, 12.5]$, $[12.5, 13.5]$ and $[13.5, 14.5]$, respectively.

quite significantly on the pair separations. Thus it is unlikely for the large scale environment to be main factor in determining the orientation of the central galaxy, otherwise one would expect θ_2 to be insensitive to the distance. On the other hand, in W08 it was found that the orientation of the central galaxy is also aligned with the potential of the HG (provided that the satellite distributions trace the mass distribution of the halo reasonably well). Therefore, we conclude both the the satellite distribution (or the mass distribution) in the HG and the NNG at small separation can affect the orientation of the central galaxy. However, from the alignment signal measured for θ_1 , we find that the distribution of the satellite is affected by both the NNG and the large scale of environment (see the last part of section 4.1), so there may be indirect correlation between the orientation of the central galaxy and the large scale environment.

In the right-hand panel of Figure 9 we show the resulting θ_2 distributions for HG-NNG systems with the mass of HG larger (filled diamond) and smaller (open diamond) than that of the NNG. The position angle of the central galaxy in more massive host group is slightly more aligned (by 1.4σ) which is very likely caused by its flatter distribution of the satellite galaxies.

To examine the dependence of the alignment signal on the group mass, we divide our sample into three subsamples according to the NNG mass as in Section 4.1. Figure 10 shows the distribution of θ_2 for systems with the NNG mass in the range $M_n \in [13.5, 14.5]$, $[12.5, 13.5]$, and $[11.5, 12.5]$ from the top to the bottom panel. The panels on the left are for the systems having a HG more massive than its NNG, and those on the right are for the opposite cases. Figure 10 clearly shows that the alignment signal is stronger for more massive systems. The statistical significance of the alignment is 3.3σ , 3.5σ , and 2.0σ from top to bottom in the left column. It is 4.0σ , 0.0σ , and 0.6σ in the same order in the right column. The top panels tell that the groups in a pair are aligned with each other when the NNG mass exceeds $10^{13.5} h^{-1} M_\odot$ regardless of the HG mass. Such align-

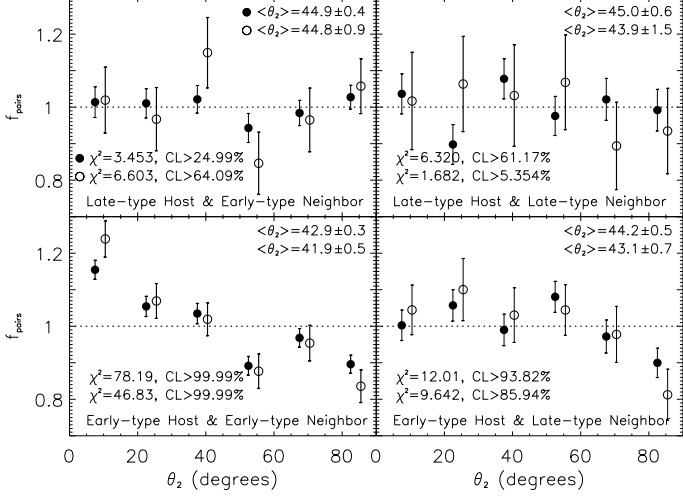


FIG. 11.— Same as Figure 9, but for different subsamples of central galaxies of the host and neighbor groups.

ment can occur by the strong tidal force of the NNG on the central galaxy of the HG. This signal due to NNGs disappears when the NNG mass is less than $10^{13.5} h^{-1} M_{\odot}$ as can be seen in the middle right and bottom right panels. Instead, the alignment signal is seen when the HG mass is higher than the NNG mass, which means that the NNG is now aligned, regardless of its mass, along the major axis of the central galaxy of the HG.

In Figure 11, we examine how $f_{\text{pairs}}(\theta_2)$ depends on the morphological type of the central galaxies. Note that the early types are mainly ellipticals, and the elongation of an early-type galaxy can be due to external gravitational effects or internal kinematics, both of which are closely correlated with the distribution of the satellite galaxies and the NNGs. On the other hand, the late types are dominantly disk galaxies and the position angle of a disk galaxy is determined by the direction of its spin axis. Therefore, for HG central galaxies with different morphological types, the alignment with respect to the NNG could have different physical origins. In the bottom two panels of Fig. 11, we show the alignment signals $f(\theta_2)$ for HGs with early-type centrals. The left panel is for the HGs whose NNG has an early-type central while the right is for those whose NNG contains a late-type central. The HGs having an early-type central show quite a strong alignment signal, particularly when the central galaxy of the NNG is also an early type (a 7σ effect for a sample of all such pairs and 6σ for close pairs). If the central galaxy of the NNG is a late type one, the alignment signal weakens considerably, the deviation from the case of no alignment is only 1.6σ and 2.7σ for all pairs and close pairs, respectively (see the lower-right panel of Figure 11).

In the case where the central galaxy of the NNG is a late type one, the major axis of the galaxy is not so well correlated with its stellar distribution, but more with the inclination of the disk. On the other hand, the minor axis is quite well correlated with the disk spin axis. Thus $\theta_2 = 0$ means that the spin axis is perpendicular to the direction of the NNG, while $\theta_2 = 90^\circ$ means that the spin axis tends to be aligned with the direction of the NNG. In the upper panels of Figure 11, we show the distribution $f(\theta_2)$ for the late type central galaxies (Upper Left:

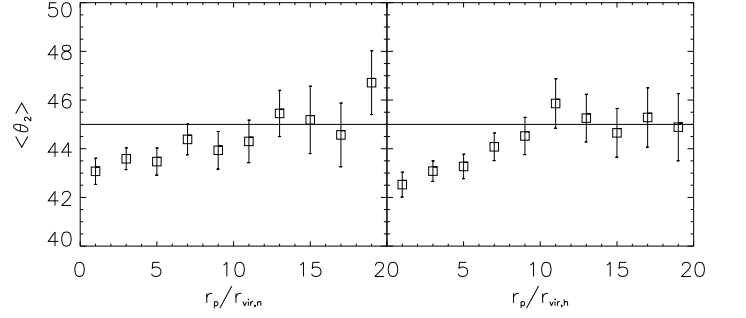


FIG. 12.— The average value of θ_2 as a function of the projected distance between the HG and the NNG. Left: as a function of $r_{\text{vir},n}$; Right: as a function of $r_{\text{vir},h}$.

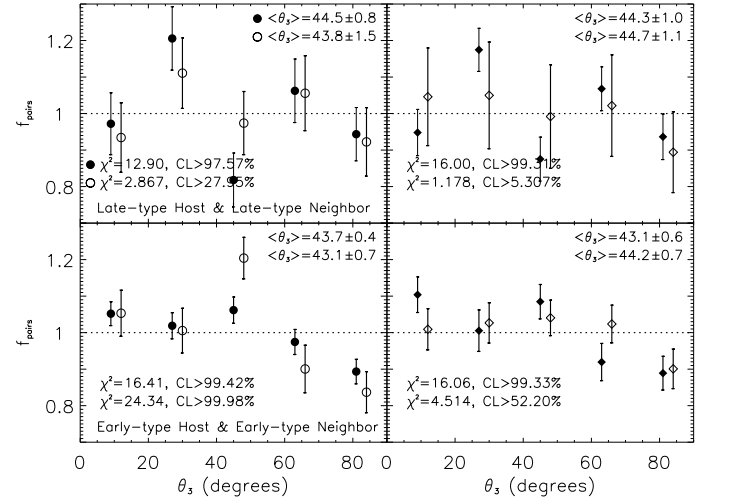


FIG. 13.— The normalized probability distribution, $f_{\text{pairs}}(\theta_3)$, of the angle θ_3 between the two major axes of the central galaxies of the HG and the NNG. Upper panels: the central galaxies of the HG and NNG are both late types. Lower panels: the central galaxies of the HG and NNG are both early types. In the two left panels we show results for the whole sample (filled circle) and the subsample with the projected distance smaller than 3 times the virial radius of the host group (open circle). In the two right panels, we show the results for subsamples where the mass of the HG are large (smaller) than that of the NNG with filled diamond (open diamond) symbol.

NNG with early type central; Upper Right: NNG with late type central). However, we do not find significant alignment signal between the major axis of the central late type galaxy and the direction of the NNGs. As we have also measured the average alignment angle $\langle \theta_2 \rangle$ as a function of distance between the HG and NNG as shown in Fig. 12, $\langle \theta_2 \rangle$ increases slowly and approaches the null position of 45° as the distance increases. The results shown in Fig. 12 indicate that only NNGs at separation $\lesssim 5r_{\text{vir}}$ may have possible impacts onto the orientations of the central galaxies in the HGs.

4.2.2. relative to the orientation of the central galaxy of the NNG

In Figure 13, we present the distribution of the angle θ_3 between the major axes of the central galaxy of the HG and the central galaxy of the NNG. In the lower panels we use only the HG and NNG whose central galaxies are both early types. One can see that the major axes of the central galaxies of the HG and the NNG tend to be parallel, though the signal is weak. We also checked the case of alignment between all types of central galaxies, and find there is no prominent signal, as shown by the fact $\langle \theta_3 \rangle = 44.6^\circ \pm 0.3^\circ$ (deviates from the null case by only 1.3σ). However, the θ_3 alignment signal for the case of the HG more massive than the NNG is stronger than the opposite case by 1.8σ (see the lower-right panel). Combined with our probe of the alignment signals for θ_1 and θ_2 , we find that the large scale environments tend to impact the distribution of satellite galaxies (and the mass distribution) in the HGs, while the distribution of satellite galaxies and possibly NNGs at small separations may impact the orientations of the (early-type) central galaxies in the HGs. Thus the alignment signals shown in θ_3 for early type galaxies are expected.

The upper panels of Figure 13 shows the distributions of θ_3 when the morphological types of the central galaxies of the HG and NNG are both late types. The spin axis of the two galaxies are parallel for $\theta_3 = 0^\circ$ and perpendicular if $\theta_3 = 90^\circ$. We find large fluctuations in the distribution, and there is no significant alignment signal between the spin axes of the late-type central galaxies, regardless whether the HG is more massive or less than the NNG.

4.3. The position angle of the satellite galaxy relative to the direction of the NNG

Many studies have attempted to detect the alignment signal between the orientations of central galaxies and satellite galaxies in the clusters of galaxies (e.g., Plionis et al. 2003; Strazzullo et al. 2005; Torlina, De Propriis & West 2007), most of them found only null or weak signal. Using a sample of 4289 host-satellites pairs from the SDSS DR4, Agustsson & Brainerd (2006) found a weak signal of the alignment. Adopting the same group catalogue as that used here, Faltenbacher et al. (2007) searched for the alignment between the orientations of the BGG and the satellites. They considered the total sample and submaples with different color of the satellite galaxy, and found a small but definite alignment signal between the major axes of the central and the satellite galaxies of the host group, especially at small scales $r_p < 0.1r_{\text{vir,h}}$, where one expects a strong tidal force at such small separation.

As we have already noticed, the NNG and the large scale environment can affect the distribution of satellite galaxies in the HG. Here, we check if the NNG (and the large scale environment) can also impact the orientation of the satellite galaxies. The method to obtain the alignment angle θ_4 is similar to that for the angle θ_3 , the only difference is that here we use the major axes of the satellites to substitute the major axis of the central galaxy of the HG. Fig. 14 shows the alignment between the major axes of the satellites in the HGs and the direction linking the host and NNGs. There is apparently no alignment between the major axes of the satellite and the direction linking the host and the NNG. Fig 15 displays the dependence on the $f_{\text{pairs}}(\theta_4)$ on the morphological type of

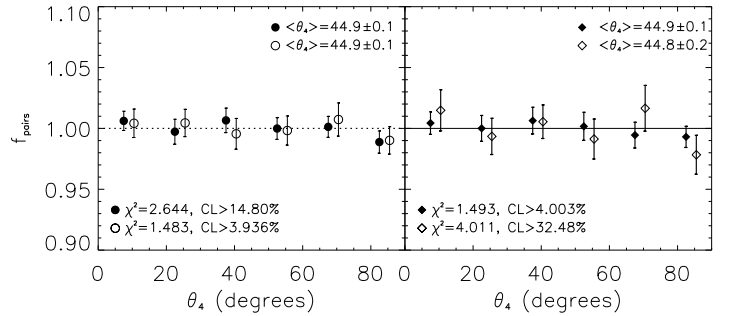


FIG. 14.— The normalized probability distribution, $f_{\text{pairs}}(\theta_4)$, of the angle θ_4 between the orientations of the satellite galaxy in HG and the direction linking the host and NNG. In the left panel, results are measured for the whole sample (solid line) and the subsample with the distance limit, 3 times the virial radius of the host group (dotted line). In the right panel, we show results for the subsamples where the mass of the HG are large (smaller) than that of the NNG with dashed (dot-dashed) line.

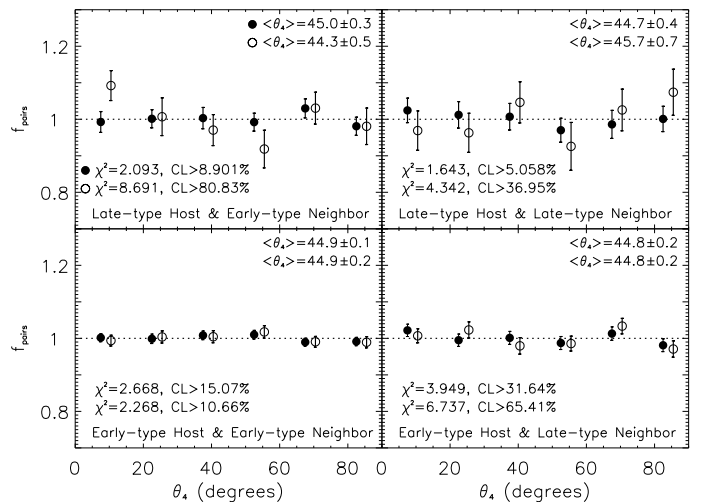


FIG. 15.— Same as Figure 14, but for subsamples of different morphological types of central galaxies of the host and neighbor groups.

the central galaxies of the HGs and NNGs. Again we do not find statistically significant alignment signal for the morphology subsamples. Moreover, we also checked the distribution $f_{\text{pairs}}(\theta_4)$ separately for the early and late type satellite galaxies, but there is no significant alignment signal either.

5. SUMMARY AND DISCUSSION

In the cold dark matter scenario, small dark matter halos form first and grow subsequently to larger structures via accretion and merger processes. The accretion of material might preferentially occur along the filamentary structure (West 1994), which leads to correlations between the internal structures of the neighboring groups. Bingeli (1982) pioneered the studies of the alignment between neighboring clusters of galaxies, and found that the host clusters tend to be aligned with their nearest neighbors. The subsequent studies confirmed this ten-

dency, although conflicting results appeared occasionally in the literature (West 1989; Plionis 1994). In this paper, we used the host-neighboring group systems extracted from the SDSS DR4 group catalogue (Yang et al. 2007) to probe the impact of the large scale environment (as represented by the nearest neighboring group) on the distribution of the satellite galaxies and on the orientation of the central and satellite galaxies. For this purpose, four types of alignment signals are measured and the main results are summarized as follows.

1. There is a strong alignment signal between the distribution of the satellites relative to the direction of the NNG. This signal is rather insensitive to the separation between the HG and NNG, and extends to separation beyond $12r_{vir}$ of the HG. For the system with both early central galaxies of the HG and NNG, the alignment signal is the strongest, for the system with both late central galaxies, the signal is weaker but still quite significant.
2. The satellite galaxies in the HG have a weak preference to be distributed at the near side of the NNG with an early type central galaxy, and at the far side of the NNG with a late type central galaxy.
3. The major axis of the central galaxy of the HG is aligned with the direction of the NNG, especially in the massive HGs. This effect is stronger for the systems when the central galaxies of HG and NNG are both early types. And we find this alignment signal only exists between HG and NNG pairs at separation $\lesssim 5r_{vir}$ of the HG.
4. The distribution of the satellite galaxies and the orientation of the central galaxy of the HG show stronger alignment signals with the NNG in systems with more massive HGs and NNGs.
5. There is a preference for the two major axes of the central galaxies of the HG and NNG to be parallel for the system with the both early central galaxies, while there is no evident correlation between the two major axes of the central galaxies for the systems with both late type central galaxies.
6. Although the distribution of the satellites of the HG is correlated with the direction of the NNG, their orientations (position angles) are not correlated with the direction of the NNG.

According to our various alignment measurements, we find that the distribution of satellite galaxies and the orientation of the central galaxy both show strong alignment signals with respect to the direction of the NNG (θ_1 and θ_2). Such alignment signals are stronger in massive halos where central galaxies are early type ones. Because of these two kinds of alignments, the alignment between the orientations of the central galaxies of the HG and the NNG (θ_3) is naturally expected. For the orientations of satellite galaxies, however, we do not find significant alignment signal relative to the direction of NNG (θ_4), while Faltenbacher et al. (2007) have found prominent alignment signals between the orientations of the central and satellite galaxies at very small separation. This may

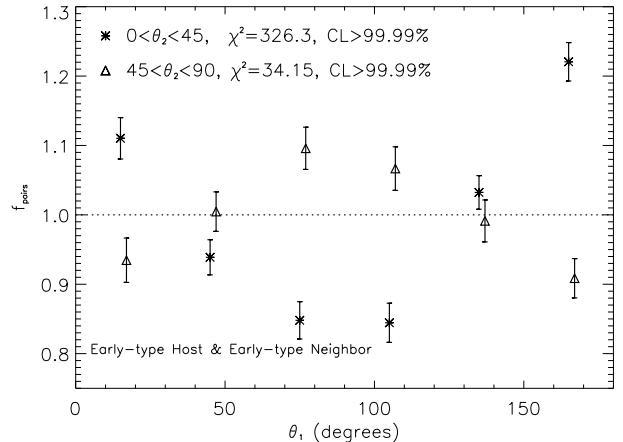


FIG. 16.— The normalized probability distribution, $f_{\text{pairs}}(\theta_1)$, of the angle θ_1 for the systems with early-type host and early-type neighbor. The asterisk and triangle symbols represent the results for the subsamples with $0^\circ < \theta_2 < 45^\circ$ and $45^\circ < \theta_2 < 90^\circ$, respectively. The triangle symbols have been shifted slightly along the horizontal axis for clarity.

indicate that the orientations of satellite galaxies are only strongly affected by the tidal force of the central galaxy and the host halo, but not significantly by the NNG or the large scale environment.

Possible explanations for the strong alignment signals in the first and second types of the alignments are: (i) the NNG affects the shape of the host halo, while the distribution of satellite galaxies and the shape of the central galaxy are mainly affected by the host halo; (ii) the large scale environment directly affects the distribution of satellite galaxies and the shape of the central galaxy. Judging from the first alignment signal, it seems likely that the impact of large scale environment is mainly on the shape of the host halo instead of directly on the distribution of the satellite galaxies, because otherwise we should expect to find a strong dependence on the distance to the NNG, rather than a mass dependence of the HG and NNG. The fact that stronger alignment signals is found for the subsamples with more massive HGs and NNGs is likely correlated with the fact that the more massive halos have larger triaxialities (e.g. Jing & Suto 2002; Wang & Fan 2004; W08).

In order to check whether the shape of the central galaxy is mainly determined/affected by its own host halo, or by the NNG at small separation, we carried out an additional test. In Fig. 16, we show the alignment signal $f_{\text{pairs}}(\theta_1)$ for the systems with the early-type host and early-type neighbor, where the asterisk and triangle symbols show the results for the system with $0^\circ < \theta_2 < 45^\circ$ and $45^\circ < \theta_2 < 90^\circ$, respectively. When $45^\circ < \theta_2 < 90^\circ$, the major axis of the central galaxy of the HG is rather perpendicular to the direction of the NNG. If the shape of central galaxy is not much affected by the host halo, but only affected by the NNG, we would expect that the alignment signals of the two subsamples are similar. The results, however, show that the alignment signals are opposite for the two different subsamples (the difference level is 7.5σ). On the other hand, the signals are precisely what one would expect if the mass and light are reasonably well-aligned (i.e., the image of early type cen-

tral galaxy and the surrounding mass of the HG) and the satellites in the HG trace the surrounding mass. That is, one would get a peak at $\theta_1 = 90^\circ$ if $45^\circ < \theta_2 < 90^\circ$ and a valley at $\theta_1 = 90^\circ$ if $0^\circ < \theta_2 < 45^\circ$. Hence, the shape and orientation of the central galaxy is more likely to be determined by its own host halo. While the different separation dependencies of $\langle \theta_2 \rangle$ shown in Figure 12 and $\langle \theta_1 \rangle$ shown in Figure 8 indicate that NNG at small separation may also play, however, only a secondary impact on the orientation of the central galaxy of the HG at particular conditions, e.g. interaction with the host halo (e.g., Lin et al. 2003; Ludlow et al. 2009). This conclusion is also strengthened by the recent measurements which show that the orientations of the central galaxies are preferentially aligned with the distribution of satellite galaxies (e.g. Y06 and references therein).

Finally, we draw our conclusion that the large scale environment traced by the NNG have impacts on the shape (orientation) of the host halo. On the other hand, the distribution of the satellite galaxies, the shapes of the central galaxies, and the shape of the satellite galaxies at small radii, however, are mainly affected by their own host halos. Apart from these, the NNG also have direct impacts on the distribution of satellite galaxies, which produce an asymmetric alignment signal with respect to the near or far away sides of the NNG. And NNG at small separations may also have small secondary impact on the orientation of the central galaxy of the HG.

ACKNOWLEDGMENTS

We thank the referee for the constructive and detailed comments and suggestions. This work has started during YGW's visit to KIAS, and he would like to express his gratitude for KIAS. CBP and YYC acknowledge the support of the Korea Science and Engineering Foundation (KOSEF) through the Astrophysical Research Center for the Structure and Evolution of the Cosmos (ARCSEC). XY acknowledges the support by

the Shanghai Pujiang Program (No. 07pj14102), 973 Program (No. 2007CB815402), the CAS Knowledge Innovation Program (Grant No. KJCX2-YW-T05) and grants from NSFC (Nos. 10533030, 10673023, 10821302). YGW and XLC acknowledges the support of the 973 program (No.2007CB815401), the CAS Knowledge Innovation Program (Grant No. KJCX3-SYW-N2), and the NSFC grant 10503010. YGW is also supported by the Young Researcher Grant of National Astronomical Observatories, Chinese Academy of Sciences. XLC is also supported by the NSFC Distinguished Young Scholar Grant No.10525314.

Funding for the SDSS and SDSS-II has been provided by the Alfred P. Sloan Foundation, the Participating Institutions, the National Science Foundation, the U.S. Department of Energy, the National Aeronautics and Space Administration, the Japanese Monbukagakusho, the Max Planck Society, and the Higher Education Funding Council for England. The SDSS Web Site is <http://www.sdss.org/>.

The SDSS is managed by the Astrophysical Research Consortium for the Participating Institutions. The Participating Institutions are the American Museum of Natural History, Astrophysical Institute Potsdam, University of Basel, Cambridge University, Case Western Reserve University, University of Chicago, Drexel University, Fermilab, the Institute for Advanced Study, the Japan Participation Group, Johns Hopkins University, the Joint Institute for Nuclear Astrophysics, the Kavli Institute for Particle Astrophysics and Cosmology, the Korean Scientist Group, the Chinese Academy of Sciences (LAMOST), Los Alamos National Laboratory, the Max-Planck-Institute for Astronomy (MPIA), the Max-Planck-Institute for Astrophysics (MPA), New Mexico State University, Ohio State University, University of Pittsburgh, University of Portsmouth, Princeton University, the United States Naval Observatory, and the University of Washington.

REFERENCES

- Adelman-McCarthy, J. K., et al. 2006, *ApJS*, 162, 38
 Agustsson, I., & Brainerd, T. G. 2006, *ApJ*, 644, L25
 Agustsson, I., & Brainerd, T. G. 2007, preprint (arXiv:0704.3441)
 Altay, G., Colberg, J. M., & Croft, R. A. C. 2006, *MNRAS*, 370, 1422
 Aragon-Calvo, M., van de Weygaert, R., & van der Hulst, T. 2006, *Proc. Bernards Cosmic Stories: From Primordial Fluctuations to the Birth of Stars and Galaxies, Meeting Abstracts*. Uimp, Valencia, Spain, p. 85.1
 Avila-Reese, V., et al. 2005, *ApJ*, 634, 51
 Azzaro, M., Patiri, S. G., Prada, F., & Zentner, A. R. 2007, *MNRAS*, 376, L43
 Bailin, J., & Steinmetz, M. 2005, *ApJ*, 627, 647
 Bailin, J., Power, C., Norberg, P., Zaritsky, D., & Gibson, B. K. 2008, *MNRAS*, 390, 1133
 Basilakos, S., Plionis, M., & Maddox, S. J. 2000, *MNRAS*, 316, 779
 Basilakos, S., Plionis, M., Yepes, G., Gottlöber, S., & Turchaninov, V. 2006, *MNRAS*, 365, 539
 Binggeli, B. 1982, *A&A*, 107, 338
 Blanton, M. R., et al. 2005, *AJ*, 129, 2562
 Brainerd, T. G. 2005, *ApJ*, 628, L101
 Brainerd, T. G., & Specian, M. A. 2003, *ApJ*, 593, L7
 Carter, D., & Metcalfe, N. 1980, *MNRAS*, 191, 325
 Colless, M., et al. (The 2dFGRS Team), 2001, *MNRAS*, 328, 1039
 Dekel, A. 1985, *ApJ*, 298, 461
 Donoso, E., O'Mill, A., & Lambas, D. G. 2006, *MNRAS*, 369, 479
 Einasto, M., Einasto, J., Müller, V., Heinämäki, P., & Tucker, D. L. 2003, *A&A*, 401, 851
 Faltenbacher, A., Gottlöber, S., Kerscher, M., & Müller, V. 2002, *A&A*, 395, 1
 Faltenbacher, A., Li, C., Mao, S., van der Bosch, F. C., Yang, X., Jing, Y. P., Pasquali, A., & Mo, H. J. 2007, *ApJ*, 662, L71
 Faltenbacher, A., Jing, Y. P., Li, C., Mao, S., Mo, H. J., Pasquali, A., & van den Bosch, F. C. 2008, *ApJ*, 675, 146
 Faltenbacher, A., Li, C., White, S. D. M., Jing, Y. P., Mao, S., & Wang, J. 2009, *RAA*, 9, 41
 Fasano, G., Pisani, A., Vio, R., & Girardi, M. 1993, *ApJ*, 416, 546
 Hahn, O., Porciani, C., Carollo, C. M., & Dekel, A. 2007a, *MNRAS*, 375, 489
 Hahn, O., Carollo, C. M., Porciani, C., & Dekel, A. 2007b, *MNRAS*, 381, 41
 Hartwick, F. D. A. 1996, in Morrison H., Sarajedini A., eds, *ASP Conf. Ser. Vol. 92, Formation of the Galactic Halo . . . Inside and Out*. Astron. Soc. Pac., San Francisco, p. 444
 Hartwick, F. D. A. 2000, *AJ*, 119, 2248
 Hawley, D. L., & Peebles, P. J. E. 1975, *AJ*, 80, 477
 Holmberg, E. 1969, *Ark. Astron.*, 5, 305
 Hopkins, P. F., Bahcall, N. A., & Bode, P. 2005, *ApJ*, 618, 1
 Jing, Y. P., & Suto, Y. 2002, *ApJ*, 574, 538
 Kang, X., van den Bosch, F. C., Yang, X., Mao, S., Mo, H. J., Li, C., & Jing, Y. P. 2007, *MNRAS*, 378, 1531
 Katgert, P., Biviano, A., & Mazure, A. 2004, *ApJ*, 600, 657
 Kasun, S. F., & Evrard, A. E. 2005, *ApJ*, 629, 781
 Knebe, A., Gill, S. P. D., Gibson, B. K., Lewis, G. F., Ibata, R. A., & Dopita, M. A. 2004, *ApJ*, 603, 7
 Knebe, A., Draganova, N., Power, C., Yepes, G., Hoffman, Y., Gottlöber, S., & Gibson, B. K. 2008a, *MNRAS*, 386, L52
 Knebe, A., Yahagi, H., Kase, H., Lewis, G., & Gibson, B. K. 2008b, *MNRAS*, 388, L34
 Koch, A., & Grebel, E. K. 2006, *AJ*, 131, 1405
 Kroupa, P., Theis, C., & Boily, C. M. 2005, *A&A*, 431, 517
 Libeskind, N. I., Frenk, C. S., Cole, S., Helly, J. C., Jenkins, A., Navarro, J. F., & Power, C. 2005, *MNRAS*, 363, 146

- Libeskind, N. I., Cole, S., Frenk, C. S., Okamoto, T., & Jenkins, A. 2007, MNRAS, 374, 16
- Lin, W. P., Jing, Y. P., & Lin, L. 2003, MNRAS, 344, 1327
- Ludlow, A. D., Navarro, J. F., Springel, V., Jenkins, A., Frenk, C. S., & Helmi, A. 2009, ApJ, 692, 931L
- Lynden-Bell, D. 1976, MNRAS, 174, 695
- Lynden-Bell, D. 1982, Observatory, 102, 202
- MacGillivray, H. T., Dodd, R. J., McNally, B. V., & Corwin H. G. Jr. 1982, MNRAS, 198, 605
- Majewski, S. R. 1994, ApJ, 431, L17
- Maulbetsch, C., Avila-Reese, V., Colin, P., Gottlöber, S., Khalatyan, A., & Steinmetz, M. 2007, ApJ, 654, 53
- McConnachie, A. W., & Irwin, M. J. 2006, MNRAS, 365, 902
- McKay, T., et al. 2002, ApJ, 571, L85
- Metz, M., Kroupa, P., & Jerjen, H. 2007, MNRAS, 374, 1125
- More, S., van den Bosch, F. C., & Cacciato, M. 2009a, MNRAS, 392, 917
- More, S., van den Bosch, F. C., Cacciato, M., Mo, H. J., Yang, X., & Li, R. 2009b, MNRAS, 392, 801
- Okumura, T., Jing, Y. P., & Li, C. 2009, ApJ, 694, 214
- Orlov, V. V., Petrova, A. V., & Tarantsev, V. G. 2001, MNRAS, 325, 133
- Park, C., & Choi, Y. -Y. 2005, ApJ, 635, L29
- Park, C., & Choi, Y. -Y. 2009, ApJ, 691, 1828
- Paz, D. J., Stasyszyn, F., & Padilla, N. D. 2008, MNRAS, 389, 1127
- Plionis, M. 1994, ApJS, 95, 401
- Plionis, M., Barrow, J. D., & Frenk, C. S. 1991, MNRAS, 249, 662
- Plionis, M., Basilakos, S., & Tovmassian, H. M. 2004, MNRAS, 352, 1323
- Plionis, M., Benoist, C., Maurogordato, S., Ferrari, C., & Basilakos, S. 2003, ApJ, 594, 144
- Plionis, M., Basilakos, S., & Ragone-Figueroa, C. 2006, ApJ, 650, 770
- Ragone-Figueroa, C., & Plionis, M. 2007, MNRAS, 377, 1785
- Sales, L., & Lambas, D. G. 2004, MNRAS, 348, 1236
- Sales, L., & Lambas, D. G. 2009, MNRAS, 395, 1184
- Sharp, N. A., Lin, D. N. C., & White, S. D. M. 1979, MNRAS, 187, 287
- Steffen, J. H., & Valenzuela, O. 2008, MNRAS, 387, 1199
- Strazzullo, V., Paolillo, M., Longo, G., Puddu, E., Djorgovski, S. G., De Carvalho, R. R., & Gal, R. R. 2005, MNRAS, 359, 191
- Struble, M. F. 1990, AJ, 99, 743
- Torlina, L., De Propris, R., & West, M. J. 2007, ApJ, 660, L97
- van den Bosch, F. C., Norberg, P., Mo, H. J., & Yang, X. 2004, MNRAS, 352, 1302
- Wang, H. Y., Jing, Y. P., Mao, S., & Kang, X. 2005, MNRAS, 364, 424
- Wang, Y. -G., & Fan, Z. -H. 2004, ApJ, 617, 847
- Wang, Y., Yang, X., Mo, H. J., Li, C., van den Bosch, F. C., Fan, Z., & Chen, X. 2008, MNRAS, 385, 1511 (W08)
- West, M. J. 1989, ApJ, 344, 535
- West, M. J. 1994, MNRAS, 268, 79
- Yang, X., Mo, H. J., van den Bosch, F. C., & Jing, Y. P. 2005, MNRAS, 356, 1293
- Yang, X., van der Bosch, F. C., Mo, H. J., Mao, S., Kang, X., Weinmann, S. M., Guo, Y., & Jing, Y. P. 2006, MNRAS, 369, 1293 (Y06)
- Yang, X., Mo, H. J., van den Bosch, F. C., Pasquali, A., Li, C., & Barden, M. 2007, ApJ, 671, 153
- Yang, X., Mo, H. J., & van den Bosch, F. C. 2009, ApJ, 695, 900
- York, D. G., et al. 2000, AJ, 120, 1579
- Zaritsky, D., Smith, R., Frenk, C. S., & White, S. D. M. 1993, ApJ, 405, 464
- Zaritsky, D., Smith, R., Frenk, C. S., & White, S. D. M. 1997, ApJ, 478, 39
- Zehavi, I., et al. 2002, ApJ, 571, 172
- Zentner, A. R., Kravtsov, A. V., Gnedin, O. Y., & Klypin, A. A. 2005, ApJ, 629, 219

APPENDIX

In this appendix, we explain how to measure the angle between the orientation of the central galaxy of the host group and NN, taking into account the effect of curvature of the sky. We take one pair of the host ($\alpha_h, \delta_h, \Phi_h$) and neighbor ($\alpha_n, \delta_n, \Phi_n$) as an example, where α_h, δ_h and Φ_h are the right ascension, declination, and the position angle of the host centrals respectively, and α_n, δ_n and δ_n are the corresponding parameters of the NN. Here we assume that $\alpha_n > \alpha_h$, $\delta_h > 0$, and $\delta_n > 0$ (See the right panel of Figure 2). Extending the major axis of the central galaxy of the NN, it will cross the longitude of the host at the point B. Now in the spherical triangle $\triangle ABC$, we have two angles $\angle BAC$ and $\angle ACB$ and one side \widehat{AC} . Therefore, we can get the angle $\angle CBA$ by solving the spherical triangle $\triangle ABC$. It is clear that the angle between the orientation of the central galaxy of the host group and NN can be written as $\Phi_h - (180^\circ - \angle CBA)$, which is equivalent to the angle $\theta_3 = \theta_{3a} - \theta_{3b}$ (see the right panel of Figure 2). Position angles of the major axes are with respect to the east direction.